

Mobile atom traps using magnetic nanowires

D. A. Allwood,^{a)} T. Schrefl, and G. Hrkac

Department of Engineering Materials, University of Sheffield, Sheffield S1 3JD, United Kingdom

I. G. Hughes and C. S. Adams

Department of Physics, University of Durham, Durham DH1 3LE, United Kingdom

(Received 27 March 2006; accepted 2 June 2006; published online 6 July 2006)

By solving the Landau-Lifshitz-Gilbert equation using a finite element method we show that an atom trap can be produced above a ferromagnetic nanowire domain wall. Atoms experience trap frequencies of up to a few megahertz, and can be transported by applying a weak magnetic field along the wire. Lithographically defined nanowire patterns could allow quantum information processing by bringing domain walls in close proximity at certain places to allow trapped atom interactions and far apart at others to allow individual addressing. © 2006 American Institute of Physics. [DOI: 10.1063/1.2219397]

Ultracold atoms make attractive candidates for quantum information processing (QIP) owing to their weak interaction with the external world. However, weak interactions also mean that it can be difficult to achieve sufficiently strong confinement, characterized by a high trap oscillation frequency ν_{trap} , for fast gate operations. For optical traps,^{1,2} increasing ν_{trap} is restricted by the simultaneous demand of minimizing spontaneous scattering. For magnetic traps, there is no such restriction and very high ν_{trap} could be used without introducing additional decoherence. In practice, achieving high ν_{trap} requires miniaturization of the magnetic trap components. Magnetic microtraps based on current carrying wires^{3,4} have been very successful but some problems remain to be solved, such as “spin flips” induced by Johnson noise in wires,^{5,6} and trapping potential variations due to current inhomogeneities along the wire.^{7–10} Considerable progress has also been made using ferromagnetic recording media^{11,12} to allow reconfigurable traps. Here, we propose an atom trap created above mobile domain walls in planar magnetic nanowires. As complex nanowire patterns can be fabricated on transparent substrates, domain wall atom traps provide a unique combination of high trap frequencies (>1 MHz; comparable to those in ion traps¹³), controlled transport, single qubit addressability, state-selective entanglement, and low decoherence. The position of domain walls in two-dimensional (2D) magnetic nanowire circuits can be controlled under moderate in-plane magnetic fields.^{14–16} So magnetic nanowire networks could be fabricated with regions where neighboring traps are sufficiently far apart to allow individual laser addressing, and other regions where traps are brought closer together to implement state-selective optically induced interactions.

Here, we consider Ni₈₁Fe₁₉ (Permalloy) nanowires of thickness $t=5$ nm and width $w=200$ nm, similar to those used in previous studies.^{16–19} These nanowires are magnetized along their length and have transverse domain walls.²⁰ The minimum energy state of a simple, straight nanowire comprises a single magnetic domain. However, domain walls can be controllably introduced to magnetic nanowires^{17,21,22} and separate regions of opposite magnetization. Figure 1(a) shows the calculated equilibrium state structure of a “head-

to-head” transverse domain wall with no applied magnetic field. A nanowire structure is discretized into tetrahedral elements, and the Landau-Lifshitz-Gilbert equation of motion and quasistatic Maxwell equations were solved using a finite element/boundary element method.²³ The domain wall stray field \mathbf{B}_{dw} is calculated analytically from equivalent dipole charges on the nanowire surface to obtain high accuracy.²⁴ The pitch of the stray field mesh above the nanowire is either 10 or 1 nm, depending on the spatial precision required.

In the region directly above the domain wall, \mathbf{B}_{dw} is dominated by the z component B_{dw}^z . A paramagnetic cooled

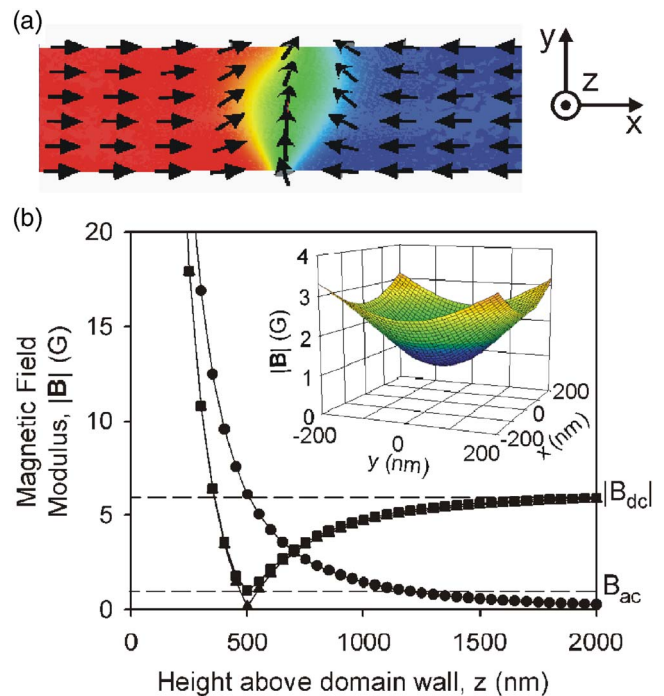


FIG. 1. (Color online) (a) Plan view of a head-to-head transverse magnetic domain wall structure within a planar magnetic nanowire calculated micromagnetically. The arrows represent magnetization direction and the color magnetization in the x direction. Also indicated are the orthogonal x , y , and z directions. (b) Calculated domain wall stray magnetic field modulus as a function of distance along the center line normal to the nanowire with no external field (●), $B_{\text{dc}}=-6.1$ G and $B_{\text{ac}}=0$ G (▲), and $B_{\text{dc}}=-6.1$ G and $B_{\text{ac}}=1$ G (■). The dotted lines show the magnitude of the externally applied fields. The inset shows a contour plot of the magnetic field modulus in the x - y plane close to an atom trap at $z=500$ nm.

^{a)}Electronic mail: d.allwood@sheffield.ac.uk

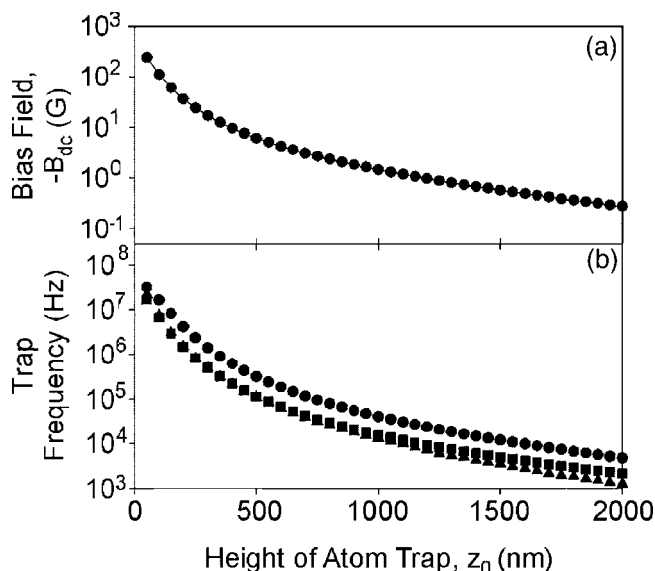


FIG. 2. (a) Required applied field bias as a function of trap height above nanowire. (b) Frequency of the domain wall atom trap in the x (\blacksquare), y (\blacktriangle), and z (\bullet) directions for a ^{87}Rb atom in the $F=2$, $m_F=2$ state as a function of trap height. Both were calculated using a 1 nm cell size.

atom in a low-field-seeking state experiences a force towards the minimum in the magnitude of magnetic field $|\mathbf{B}|$. For the case of domain wall stray field only, $|\mathbf{B}_{\text{dw}}|$ decreases with distance above the nanowire [Fig. 1(b)], and an atom would be repelled from the domain wall. However, if a uniform out-of-plane magnetic field B_{dc} is also applied to the system, B_{dw}^2 will be exactly compensated over a three-dimensional (3D) surface above the domain wall. A point will exist on this surface, and close to the $x=y=0$ line, where the x and y components of magnetic field are also zero, so that the field magnitude minimum $|\mathbf{B}|_{\text{min}}=0$ [Fig. 1(b)]. However, $|\mathbf{B}|_{\text{min}} > 0$ is required in order to preserve the low-field-seeking angular momentum atomic state. This can be achieved by additionally applying a rotating magnetic field of amplitude B_{ac} , as in a conventional time-orbiting potential trap.^{25,26} Provided the frequency of the rotating field exceeds ν_{trap} but is less than the Larmor precession frequency $\nu_L = \mu_B |\mathbf{B}|_{\text{min}} / \hbar$, trapped atoms will respond to the time averaged field modulus. Then, $|\mathbf{B}|_{\text{min}} = B_{\text{ac}}$, $|\mathbf{B}| = |B_{\text{dc}}|$ at long distances from the domain wall, and so the trap depth, $B_{\text{trap}} = |B_{\text{dc}}| - B_{\text{ac}}$ [Fig. 1(b)]. This also requires that for a particular trap height, B_{ac} must be above a critical value to ensure that $\nu_L > \nu_{\text{trap}}$. The domain wall trap is analogous to the atom traps formed above current carrying wires³ except that for the domain wall case, the trap is zero-dimensional (0D) rather than quasi-one-dimensional (quasi-1D). The external fields required to create a field minimum at reasonable distances from the domain wall are relatively small [Fig. 2(a)]. For instance, for a ^{87}Rb atom with angular momentum quantum numbers $F=2$ and $m_F=+2$, applying $B_{\text{dc}}=-6.1$ G and $B_{\text{ac}}=1$ G will create a field minimum at a height $z_0=500$ nm with a trap depth equivalent to a temperature of $340 \mu\text{K}$. The spin-flip loss rate calculated from the ratio of the spin-flip energy ($2\mu_B |\mathbf{B}|_{\text{min}}$) to the vibrational energy²⁷ is negligibly small for the above parameters. Thermal fluctuations in metallic films close to trapped atoms can also cause spin relaxation.²⁸ We calculate that this effect will limit the lifetime of a trap with $z_0=500$ nm and $\nu_{\text{trap}}=1$ MHz above the nanowire considered here to ~ 20 s. In this case, the trap lifetime would become

limited by the quality of the operating vacuum.

The trap frequency for each dimension as a function of the trap height is shown in Fig. 2(b) for $B_{\text{ac}}=1$ G. For $z_0=500$ nm, $\nu_x=\nu_y \sim 110$ kHz, and $\nu_z=320$ kHz, giving a mean trap frequency, $\bar{\nu}=(\nu_x\nu_y\nu_z)^{1/3}=160$ kHz. For $z_0=250$ nm, $\bar{\nu}$ increases to 1.2 MHz, significantly higher than can be achieved in other atom systems, while B_{ac} must increase to 2 G to ensure $\nu_L > \bar{\nu}$. $\bar{\nu}$ can be increased further by increasing the nanowire cross-sectional area, although this will eventually change the domain wall structure into a vortex,²⁰ altering the position of $|\mathbf{B}|_{\text{min}}$.

One benefit of the geometry used here is that a single bias field plus a rotating field will create the necessary trap conditions throughout a 2D nanowire network, independent of in-plane wire direction. However, if QIP is to be achieved with an array of domain wall atom traps, additional in-plane fields are required to propagate the domain walls through the nanowires. These fields shift the position of atom traps relative to domain walls. For example, with no in-plane quasi-static field and $B_{\text{dc}}=-20$ G, the trap position (x,y,z) is $(0,70,280)$ nm. With the addition of a field, $B_{\text{app}}^x=20$ G in the x direction, the trap moves to $(-170,70,170)$ nm. Alternatively, if B_{app}^x is removed and replaced by the transverse field $B_{\text{app}}^y=20$ G in the y direction, the trap is located at $(0,-100,170)$ nm. With an additional in-plane field B_{app} in either the x or y direction, the trap depth increases to $B_{\text{trap}}=(B_{\text{dc}}^2+B_{\text{app}}^2)^{1/2}-B_{\text{ac}}$, so for the above conditions, B_{app} increases the trap depth from 1.3 to 1.8 mK. This is accompanied by a doubling of $\bar{\nu}$. These calculations simplify the experimental situation by assuming that the domain wall structure remains unaffected by the externally applied fields.

The finite depth of the domain wall atom traps places an upper limit on trap and domain wall acceleration before trapped atoms are lost. For parameters corresponding to Fig. 1, the maximum acceleration is $6.4 \times 10^4 \text{ m s}^{-2}$. Domain walls propagating under steady-state conditions typically accelerate to their drift velocity in ~ 1 ns.²⁹ However, the acceleration experienced by a trapped atom will be averaged over the trap period, so for megahertz trap frequencies the domain wall drift velocities will be limited to a few cm s^{-1} . Average domain wall velocities of 0.01 m s^{-1} have been measured¹⁹ in a nanowire similar to that considered here. This velocity might be reduced further by introducing periodic defects in the wire edges. This has been demonstrated previously using ultrathin nanowires with out-of-plane magnetization to reliably lower domain wall velocities by two orders of magnitude.³⁰

In order to extend this concept of a domain wall atom trap to a vehicle for QIP, single qubit rotations of individual atoms in separate traps and state-selective interactions between atoms in neighboring traps are required. Figure 3 illustrates a nanowire network of isolated 2D nanowires that is designed to perform both qubit rotations and interactions. Two network ‘‘tiles’’ are shown that can be tessellated to create networks for large numbers of qubits. Domain walls can be introduced to the nanowires with magnetically soft ‘‘injection pads’’^{21,22} and propagated through the individual nanowires using an appropriate sequence of in-plane magnetic fields. The central region of the tiles has curved track sections of two different radii so that domain walls in adjacent tracks will come into close proximity under a field applied in the y direction (Fig. 3). This allows accurate control

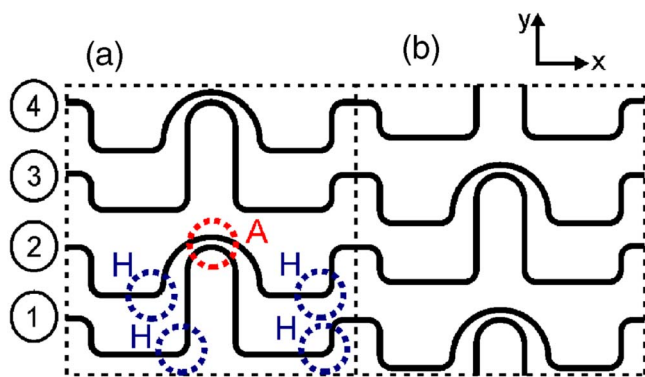


FIG. 3. (Color online) Proposed magnetic nanowire “tile” network to allow optical addressing of individual atom traps in some regions and interaction between trapped atoms in others. The two dotted square tiles each contain a design of magnetic nanowires that may be tessellated to create larger structures with full interaction between a large number of atom traps. The dotted circles are example regions of where optically induced Hadamard operations (H) or atomic interactions (A) may be performed.

of the phase shift accumulated during the state-selective interaction. Due to the alternating curve radius of the nanowire tracks, any number of qubits can in principle undergo complete interaction given a sufficient number of tile tessellations. Atoms are loaded into a 1D array of domain wall traps using a large period optical lattice (far left of Fig. 3) and initialized in a sequence of 0’s, 1’s, or superposition states using stimulated Raman transitions. When the qubits are brought close to their neighbors in the central tile regions, state-selective coupling between channels can be implemented either using cavity quantum electrodynamics³¹ (QED) or the dipole-blockade mechanism.³² Following this, atoms can be moved to the next tile or back to their initial position to perform additional rotations or readout. Combining these operations it is straightforward to realize a universal gate: for example, a Hadamard rotation on channel 1 could create a superposition state, and channel 2 initialized in state $|0\rangle$ or $|1\rangle$ as required. In the center of a tile, the coupling field introduces a phase shift to the superposition state in channel 1 that is conditional on the state in channel 2. Finally, when the atoms reach the other side of the tile, a second Hadamard operation on channel 1 completes a controlled NOT operation.

This example scheme is not without its uncertainties. For example, we have not yet considered how bringing two domain walls together will be affected by their structure or how their proximity will affect the trapping of two atoms. An alternative scheme in which atoms are brought together at nanowire junctions similar to those used in domain wall logic¹⁶ would initially appear attractive. However, previous work³³ suggests that two domain walls join together when propagating across a junction, which could result in the ejection of one of the trapped atoms.

In conclusion, we have shown that field minima produced above domain walls in magnetic nanowires provide a combination of tight atom confinement with controlled motion making this a promising system for QIP.

The authors thank E. A. Hinds and R. P. Cowburn for stimulating discussions. One of the authors (D.A.A.) acknowledges the EPSRC for financial support.

- ¹O. Mandel, M. Greiner, A. Widera, T. Rom, T. W. Hänsch, and I. Bloch, *Nature (London)* **425**, 937 (2003).
- ²M. Trupke, F. Ramirez-Martinez, E. A. Curtis, J. P. Ashmore, S. Eriksson, E. A. Hinds, Z. Moktadir, C. Gollasch, M. Kraft, G. Vijaya Prakash, and J. J. Baumberg, *Appl. Phys. Lett.* **88**, 071116 (2006).
- ³R. Folman, P. P. Kruger, J. Schmiedmayer, J. J. Denschlag, and C. Henkel, *Adv. At., Mol., Opt. Phys.* **48**, 263 (2002).
- ⁴S. Groth, P. Krüger, S. Wildermuth, R. Folman, T. Fernholz, J. Schmiedmayer, D. Mahalu, and I. Bar-Joseph, *Appl. Phys. Lett.* **85**, 2980 (2004).
- ⁵M. P. A. Jones, C. J. Vale, D. Sahagun, B. V. Hall, and E. A. Hinds, *Phys. Rev. Lett.* **91**, 080401 (2003).
- ⁶D. M. Harber, J. M. McGuirk, J. M. Obrecht, and E. A. Cornell, *J. Low Temp. Phys.* **133**, 229 (2003).
- ⁷A. E. Leanhardt, Y. Shin, A. P. Chikkatur, D. Kielpinski, W. Ketterle, and D. E. Pritchard, *Phys. Rev. Lett.* **90**, 100404 (2003).
- ⁸J. Fortagh, H. Ott, S. Kraft, A. Gunter, and C. Zimmermann, *Phys. Rev. A* **66**, 041604(R) (2002).
- ⁹D. W. Wang, M. D. Lukin, and E. Demler, *Phys. Rev. Lett.* **92**, 076802 (2004).
- ¹⁰J. Esteve, T. Schumm, C. Figl, D. Mailly, I. Bouchoule, C. I. Westbrook, and A. Aspect, *Phys. Rev. A* **70**, 043629 (2004).
- ¹¹E. A. Hinds and I. G. Hughes, *J. Phys. D* **32**, R119 (1999).
- ¹²S. Eriksson, F. Ramirez-Martinez, E. A. Curtis, B. E. Sauer, P. W. Nutter, E. W. Hill, and E. A. Hinds, *Appl. Phys. B: Lasers Opt.* **79**, 811 (2004).
- ¹³F. Schmidt-Kaler, H. Höffner, M. Riebe, S. Gulde, G. P. T. Lancaster, T. Deuschle, C. Becher, C. F. Roos, J. Eschner, and R. Blatt, *Nature (London)* **422**, 408 (2003).
- ¹⁴X. Zhu, D. A. Allwood, G. Xiong, R. P. Cowburn, and P. Grütter, *Appl. Phys. Lett.* **87**, 062503 (2005).
- ¹⁵A. Yamaguchi, T. Ono, S. Nasu, K. Miyake, K. Mibu, and T. Shinjo, *Phys. Rev. Lett.* **92**, 077205 (2003).
- ¹⁶D. A. Allwood, G. Xiong, C. C. Faulkner, D. Atkinson, D. Petit, and R. P. Cowburn, *Science* **309**, 1688 (2005).
- ¹⁷A. Himeno, T. Ono, S. Nasu, K. Shigeto, K. Mibu, and T. Shinjo, *J. Appl. Phys.* **93**, 8430 (2003).
- ¹⁸D. A. Allwood, G. Xiong, and R. P. Cowburn, *Appl. Phys. Lett.* **85**, 2848 (2004).
- ¹⁹D. Atkinson, D. A. Allwood, G. Xiong, M. D. Cooke, C. C. Faulkner, and R. P. Cowburn, *Nat. Mater.* **2**, 85 (2003).
- ²⁰R. D. McMichael and M. J. Donahue, *IEEE Trans. Magn.* **33**, 4167 (1997).
- ²¹K. Shigeto, T. Shinjo, and T. Ono, *Appl. Phys. Lett.* **75**, 2815 (1999).
- ²²M. T. Bryan, D. Atkinson, and D. A. Allwood, *Appl. Phys. Lett.* **88**, 032505 (2006).
- ²³T. Schrefl, M. E. Schabes, D. Suess, and M. Stehno, *IEEE Trans. Magn.* **40**, 2341 (2004).
- ²⁴M. Rech, Diplomarbeit thesis, Rheinischen Friedrich-Wilhelms-Universität, 2002.
- ²⁵W. Petrich, M. H. Anderson, J. R. Ensher, and E. A. Cornell, *Phys. Rev. Lett.* **74**, 3352 (1995).
- ²⁶M. H. Anderson, J. R. Ensher, M. R. Matthews, C. E. Wieman, and E. A. Cornell, *Science* **269**, 198 (1995).
- ²⁷C. V. Sukumar and D. M. Brink, *Phys. Rev. A* **56**, 2451 (1997).
- ²⁸S. Scheel, P. K. Rekdal, P. L. Knight, and E. A. Hinds, *Phys. Rev. A* **72**, 042901 (2005).
- ²⁹Y. Nakatani, A. Thiaville, and J. Miltat, *Nat. Mater.* **2**, 521 (2003).
- ³⁰F. Cayssol, D. Ravelosona, C. Chappert, J. Ferrè, and J. P. Jamet, *Phys. Rev. Lett.* **92**, 107202 (2004).
- ³¹T. Sleator and H. Weinfurter, *Phys. Rev. Lett.* **74**, 4087 (1995).
- ³²D. Jaksch, J. I. Cirac, P. Zoller, S. L. Rolston, R. Côté, and M. D. Lukin, *Phys. Rev. Lett.* **82**, 2208 (2000).
- ³³C. C. Faulkner, D. A. Allwood, M. D. Cooke, G. Xiong, D. Atkinson, and R. P. Cowburn, *IEEE Trans. Magn.* **39**, 2860 (2003).